Laser dynamics in sawtooth-like self-mixing signals

Rapahaël Teysseyre, Francis Bony, Julien Perchoux, Thierry Bosch

Laser dynamics in sawtooth-like self-mixing signals

Raphael Teysseyre,[1,2,3,*] Francis Bony,[2,3] Julien Perchoux,[2,3] and Thierry Bosch[2,3]

[1]*Epsiline, 27 rue d'Aubuisson, F-31000 Toulouse, France*

[2]*CNRS, LAAS, 7 Avenue du Colonel Roche, F-31077 Toulouse Cedex 4, France*

[3]*Université de Toulouse; UPS, INSA, INPT, ISAE, UT1, UTM, LAAS, F-31077 Toulouse Cedex 4, France*

**Corresponding author: rteysseyre@epsiline.com*

Received May 25, 2012; revised July 12, 2012; accepted July 20, 2012;
posted July 23, 2012 (Doc. ID 169352); published September 5, 2012

In this Letter, we experimentally show that transient phenomenons in self-mixing signals from a moving target contain information about the target reflectivity and distance. These transient phenomenons are well explained with a dynamical model of the laser diode, which is used to trace an abacus giving the target reflectivity and distance from a measured high-bandwidth, self-mixing signal.

OCIS codes: 140.5960, 280.3420.

In this Letter, we are considering the relaxation dynamics of a long external cavity in the case of a sawtooth self-mixing signal obtained with a rotating target for sensing purpose. The behavior of a laser diode under feedback can be described by coupled delayed differential equations [1,2]:

$$\frac{dn(t)}{dt} = \frac{I}{eV} - \frac{n(t)}{\tau_e} - g v_g \frac{S(t)}{V}, \tag{1}$$

$$\frac{dS(t)}{dt} = \frac{S(t)}{\tau_{ph}}(g/g_{th} - 1) + \frac{2\zeta}{\tau_{in}}\sqrt{S(t)S(t-\tau_{ext})} \cdot \cos(\omega_{th}\tau_{ext} + \phi(t) - \phi(t-\tau_{ext})), \tag{2}$$

$$\frac{d\phi(t)}{dt} = \frac{\alpha v_g}{2}\frac{\partial g}{\partial n}(n(t) - n_{th}) - \frac{\zeta}{\tau_{in}}\sqrt{\frac{S(t-\tau_{ext})}{S(t)}} \cdot \sin(\omega_{th}\tau_{ext} + \phi(t) - \phi(t-\tau_{ext})), \tag{3}$$

where $n(t)$, $S(t)$ and $\phi(t)$ are respectively the carrier density, the number of photons and the phase of the field inside the cavity of the laser diode, I is the injection current, τ_e, τ_{ph}, τ_{in} and τ_{ext} are the carrier lifetime, the photon lifetime, the round-trip flight time inside the cavity and the round-trip flight time to the target. g_{th}, n_{th} and ω_{th} are the gain, the carrier density and the optical pulsation at the laser threshold, α is the linewidth enhancement factor, and v_g is the group velocity inside the cavity. V is the active volume of the cavity. e and c are respectively the electron charge and the speed of light in vacuum. Finally, $g \propto n(t) - n_{th}$ is the optical gain, and $\zeta = \frac{r_3}{r_2}(1 - r_2^2)$ describes the coupling between the laser cavity and the target: r_2 is the amplitude reflectivity of the output mirror of the cavity, and r_3 is the effective reflectivity of the target, taking into account the insertion losses in the laser cavity.

These equations can be simplified to a steady-state model generally used in sensing applications [2–6], by using $dn/dt = 0$, $dS/dt = 0$ and $d\phi/dt = \omega - \omega_{th}$. In the moderate feedback regime, there are several solutions to the steady-state equations thus obtained, and a change in the laser-to-target distance can lead to a bifurcation in the set of solutions, inducing a discontinuity in the modelled power of the laser diode (Fig. 1).

To better understand what happens at these discontinuities, we set up an experiment that allows a wide range of round-trip time τ_{ext} and reflectivity r_3, with a high-bandwidth acquisition system. In this experiment (Fig. 2), the beam from a Hitachi HL7851 LD is collimated and injected into an optical delay line. This delay line is made with a 90° prism that can be continuously moved along a graduated, four-meter-long optical rail while keeping its alignment. Because the beam is well-collimated in the delay line, its only effect is to lengthen the round-trip time of flight to the target by up to 25 ns, with an accuracy of 7 ps (the total round-trip time of flight is then known with an accuracy of 20 ps).

After its extraction from the delay line, the laser beam is focused on a microprism-coated rotating target, which leads to a high r_3 coefficient that can be reduced with a variable attenuator. The effect of speckle is reduced by selecting only the biggest fringes in the self-mixing signal. The laser diode is powered by a constant 120 mA current source, and a 90 MHz bandwidth transimpedance amplifier extracts the measured optical power from the monitoring photodiode included in the laser diode package.

For low r_3, this experiment shows the quasi-sinusoidal signal predicted by the steady-state model when it has only one solution. For very high r_3, the laser diode becomes expectedly unstable. In between the two, however, the output power of the laser diode shows high-frequency damped oscillations where the steady-state model predicts discontinuities. The classically observed waveform can be retrieved by applying a low-pass filter on the signal (Fig. 3). The period of the damped oscillations varies linearly with τ_{ext}, with an offset that depends on r_3 (Fig. 4).

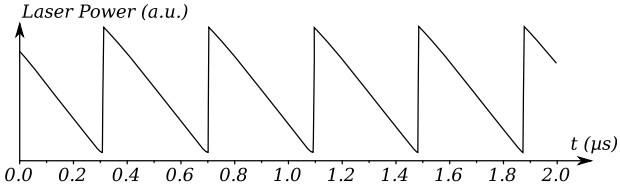

Fig. 1. Typical steady-state simulation in the moderate feedback regime for a target moving at 1 m/s.

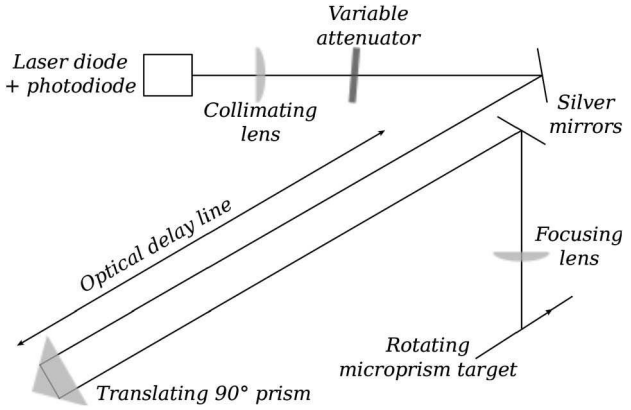

Fig. 2. Schematic of the experimental setup.

In typical applications, the target is less than a meter away from the laser diode: This leads to a round-trip time of flight of less than 7 ns. Therefore, according to Fig. 4, an acquisition system with at least 100 MHz of bandwidth is required to observe these damped oscillations. Such a bandwidth is not useful for most applications. To the authors knowledge, these oscillations so far have not been observed in self-mixing-based sensors.

The description of the observed behavior needs the complete dynamical model of Eqs. (1)–(3). Solving these equations with a fourth-order Runge-Kutta solver results in damped oscillations that behave as the ones seen in the experiment (Fig. 5).

To get a more detailed view of the relationship between τ_{ext}, r_3 and the characteristics of the damped oscillations, we have to study Eqs. (1)–(3) more closely. If we suppose that the laser diode is close to a steady state, we write:

$$(n(t), S(t), \omega(t)) = (n_0, S_0, \omega_0) + (\Delta n(t), \Delta S(t), \Delta\omega(t)), \tag{4}$$

with (n_0, S_0, ω_0) a steady-state solution of Eqs. (1)–(3), and $(\Delta n, \Delta S, \Delta\omega) \ll (n_0, S_0, \omega_0)$ a small variation around this steady state. We also need the phase modification induced by $\Delta\omega$ on a round trip to the target to be small, i.e., $\int_{t-\tau_{\text{ext}}}^{t} \Delta\omega(T)\mathrm{d}T \ll \pi$. By using first-order approximations, it is then possible to linearize the dynamic equations. We then suppose that:

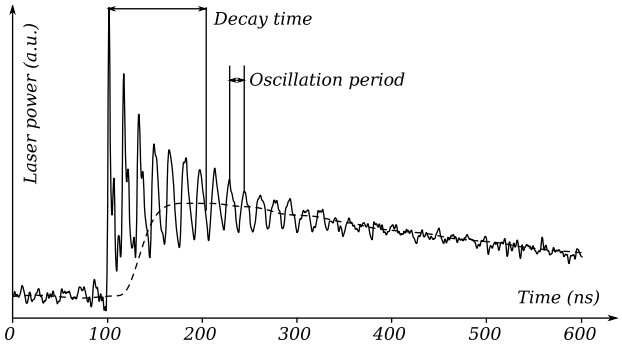

Fig. 3. Solid: measured time series of a typical signal for a medium r_3 ($\tau_{\text{ext}} = 14.9$ ns, averaging on 512 acquisitions). Dashed: the same signal, filtered.

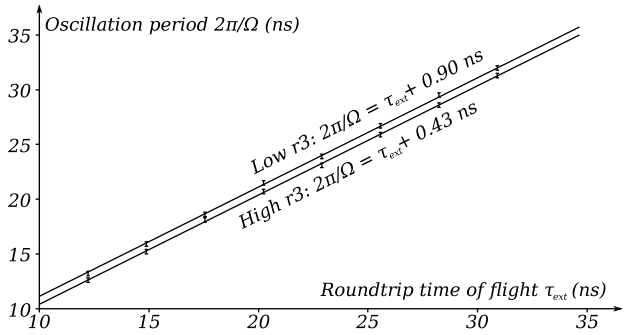

Fig. 4. Measured period of the damped oscillations versus time of flight to the target, for a tenfold variation of r_3, fitted by a least square method.

$$\Delta X = \Delta X_0 e^{j(\Omega t + \varphi_X)} e^{-t/\tau}, \tag{5}$$

with $X = n, S$ or ω, ΔX_0 being the amplitude at $t = 0$ and φ_X the phase of n, S or ω. Thus, we can derive an equation giving the pulsation of oscillations Ω and their decay time τ:

$$1 = \frac{\alpha v_g a}{2} \frac{\Delta n_0 e^{j\varphi_n}}{\Delta\omega_0 e^{j\varphi_\omega}} + \frac{\zeta}{\tau_L}(1 - e^{\tau_{\text{ext}}/\tau - j\Omega\tau_{\text{ext}}}) \cdot \left(\frac{1}{2S_0} \frac{\Delta S_0 e^{j\varphi_S}}{\Delta\omega_0 e^{j\varphi_\omega}} \sin(\omega_0\tau_{\text{ext}}) - \frac{\cos(\omega_0\tau_{\text{ext}})}{j\Omega - 1/\tau}\right), \tag{6}$$

with

$$\frac{\Delta\omega_0 e^{j\varphi_\omega}}{\Delta S_0 e^{j\varphi_S}} = \left[\frac{1}{\tau} - j\Omega + \frac{g_0/g_{\text{th}} - 1}{\tau_{\text{ph}}} + \frac{aS_0}{\tau_{\text{ph}} g_{\text{th}}} \frac{\Delta n_0 e^{j\varphi_n}}{\Delta S_0 e^{j\varphi_S}} + \frac{\zeta}{\tau_L}(1 + e^{\tau_{\text{ext}}/\tau - j\Omega\tau_{\text{ext}}})\cos(\omega_0\tau_{\text{ext}})\right] \cdot \left[\frac{2\zeta}{\tau_L} \frac{S_0}{j\Omega - 1/\tau}(1 - e^{\tau_{\text{ext}}/\tau - j\Omega\tau_{\text{ext}}})\sin(\omega_0\tau_{\text{ext}})\right]^{-1},$$

$$\frac{\Delta n_0 e^{j\varphi_n}}{\Delta S_0 e^{j\varphi_S}} = \frac{-g_0}{\frac{V}{v_g}(j\Omega - 1/\tau + 1/\tau_e) + aS_0},$$

where $a = \frac{\partial g}{\partial n}$ and g_0 is the optical gain for $n = n_0$. By numerically solving Eq. (6) with typical laser diode parameters [7], we have been able to draw an abacus

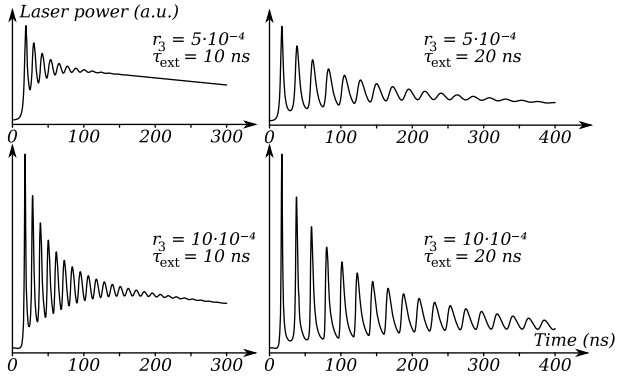

Fig. 5. Simulated signal in the dynamical model for two different r_3 and τ_{ext}. Compare with Fig. 3.

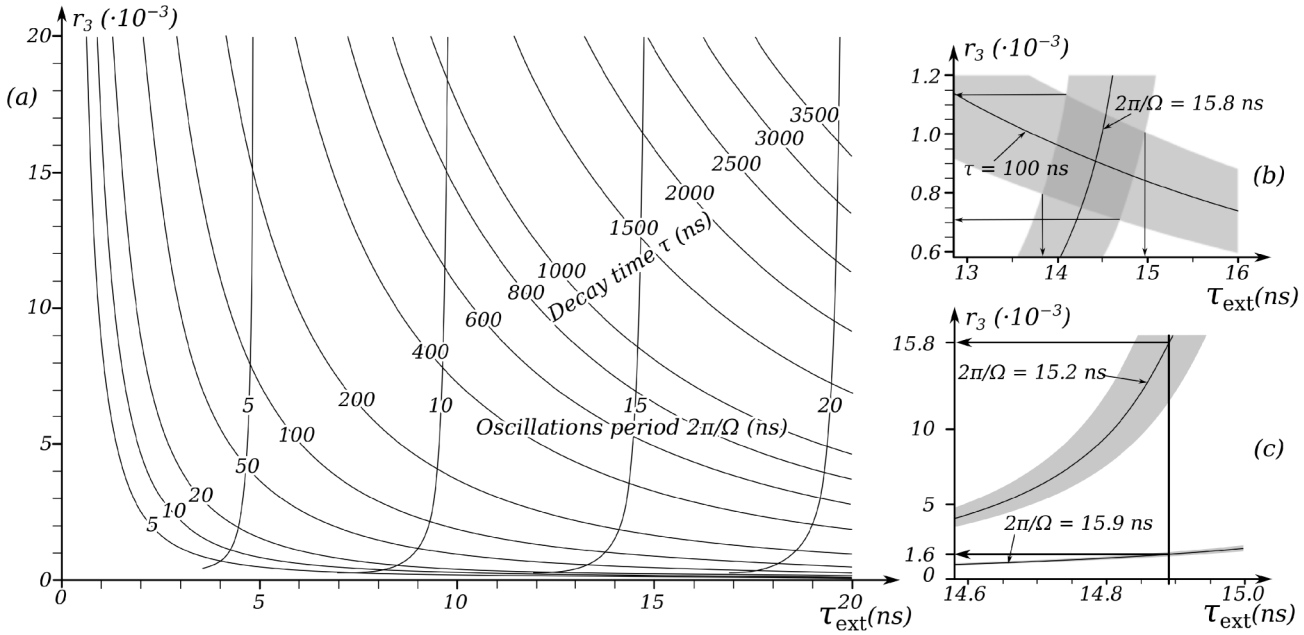

Fig. 6. (a) Abacus giving the oscillations period $2\pi/\Omega$ and decay time τ versus τ_{ext} and r_3. (b) Using the abacus with experimental data corresponding to Fig. 3 to estimate τ_{ext} and r_3. (c) Using the abacus with the data points at 14.89 ns in Fig. 4 to evaluate a ratio of r_3. The gray areas represent uncertainties on the experimental data.

[Fig. 6(a)] giving $2\pi/\Omega$ and τ versus τ_{ext} and r_3 for the oscillations occurring right after a discontinuity in the steady-state. This abacus confirms the behavior seen experimentally and by numerically solving the dynamical equations: The oscillations' period $2\pi/\Omega$ varies linearly with τ_{ext} with an offset that depends on r_3, and the decay time τ increases with r_3 and τ_{ext}. Figures 6(b) and 6(c) are zoomed-in versions of Fig. 6(a), which are used to illustrate how experimental and theoretical data have been cross-checked.

The high-frequency component in Fig. 3 is well fitted (using a least square algorithm), until the decay into noise at 350 ns, by a damped cosine (5) with a period of $2\pi/\Omega = 15.8 \pm 0.5$ ns and a decay time of $\tau = 100 \pm 20$ ns.

The high-frequency component in Fig. 3 is well fitted (using a least square algorithm), until the decay into noise at 350 ns, by a damped cosine (5) with a period of $2\pi/\Omega = 15.8 + 0.5$ ns and a decay time of $\tau = 100 \pm 20$ ns.To illustrate the possible use of the abacus, these values are reported on the abacus of Fig. 6(b): The experimental data (black curves) with its uncertainties (light gray) encloses an area (deeper gray) in the (τ_{ext}, r_3)-plane. The extent of this area tells that $13.8 \text{ ns} < \tau_{ext} < 15$ ns, and $0.7 \cdot 10^{-3} < r_3 < 1.15 \cdot 10^{-3}$ (black arrows). This is consistent with the experimental measurement of $\tau_{ext} = 14.9 \pm 0.02$ ns.

In Fig. 4, the two data points at $\tau_{ext} = 14.89$ ns give $2\pi/\Omega = 15.2 \pm 0.05$ ns for the low r_3, and $2\pi/\Omega = 15.9 \pm 0.05$ ns for the high one. These values are reported in Fig. 6(c) (black curves), with their uncertainties (gray areas). The vertical line at $\tau_{ext} = 14.89$ ns crosses these curves at $r_3 = 15.8$ and $r_3 = 1.6$, respectively, which is consistent with the tenfold ratio of r_3 between the two data points. Similar validation has been performed for all the experimental data points shown in Fig. 4

Damped oscillations in sawtooth-like self-mixing signal contain information on the target distance and reflectivity. We have shown these oscillations experimentally, and we have mapped the characteristics of these damped oscillations to the target distance and reflectivity. We have shown it is possible to estimate a target distance and reflectivity from the same self-mixing signal typically used to compute its motion.

References

1. K. Petermann, *Laser Diode Modulation and Noise* (Springer, 1991).
2. G. A. Acket, D. Lenstra, A. J. Den Boef, and B. H. Verbeek, IEEE J. Quantum Electron. **20**, 1163 (1984).
3. R. Kliese, Y. L. Lim, T. Bosch, and A. D. Rakic, Opt. Lett. **35**, 814 (2010).
4. F. P. Mezzapesa, A. Ancona, T. Sibillano, F. De Lucia, M. Dabbicco, P. Mario Lugarà, and G. Scamarcio, Opt. Lett. **36**, 822 (2011).
5. U. Zabit, O. Bernal, T. Bosch, and F. Bony, Opt. Lett. **36**, 612 (2011).
6. M. Norgia, G. Guiliani, and S. Donati, IEEE Trans. Instrum. Meas. **56**, 1894 (2007).
7. D. M. Kane and K. A. Shore, *Unlocking Dynamical Diversity* (Wiley, 2005).